HHS Public Access

Author manuscript

AJR Am J Roentgenol. Author manuscript; available in PMC 2015 December 15.

Published in final edited form as:

AJR Am J Roentgenol. 2015 November ; 205(5): 1075–1085. doi:10.2214/AJR.14.13970.

Performance of Apparent Diffusion Coefficient Values and Conventional MRI Features in Differentiating Tumefactive Demyelinating Lesions From Primary Brain Neoplasms

Marc C. Mabray[1], **Benjamin A. Cohen**[1], **Javier E. Villanueva-Meyer**[1], **Francisco E. Valles**[1], **Ramon F. Barajas**[1], **James L. Rubenstein**[2], and **Soonmee Cha**[1]

[1]Department of Radiology and Biomedical Imaging, University of California at San Francisco, 350 Parnassus Ave, Box 0336, Ste 307H, San Francisco, CA 94143-0628

[2]Department of Medicine, Division of Hematology/Oncology, University of California at San Francisco, San Francisco, CA

Abstract

OBJECTIVE—Tumefactive demyelinating lesions (TDLs) remain one of the most common brain lesions to mimic a brain tumor, particularly primary CNS lymphoma (PCNSL) and high-grade gliomas. The purpose of our study was to evaluate the ability of apparent diffusion coefficient (ADC) values and conventional MRI features to differentiate TDLs from PCNSLs and high-grade gliomas.

MATERIALS AND METHODS—Seventy-five patients (24 patients with TDLs, 28 with PCNSLs, and 23 with high-grade gliomas) with 168 brain lesions (70 TDLs, 68 PCNSLs, and 30 high-grade gliomas) who underwent DWI before surgery or therapy were included in the study. Minimum ADC (ADC_{min}) and average ADC (ADC_{avg}) values were calculated for each lesion. ANOVA and ROC analyses were performed. ROC analyses were also performed for the presence of incomplete rim enhancement and for the number of lesions. Multiple-variable logistic regression with ROC analysis was then performed to evaluate performance in multiple-variable models.

RESULTS—ADC_{min} was statistically significantly higher ($p < 0.01$) in TDLs (mean, 0.886; 95% CI, 0.802–0.931) than in PCNSLs (0.547; 95% CI, 0.496–0.598) and high-grade gliomas (0.470; 95% CI, 0.385–0.555). (All ADC values in this article are reported in units of $\times 10^{-3}$ mm^2/s.) ADC_{avg} was statistically significantly higher ($p < 0.01$) in TDLs (mean, 1.362; 95% CI, 1.268–1.456) than in PCNSLs (0.990; 95% CI, 0.919–1.061) but not in high-grade gliomas (1.216; 95% CI, 1.074–1.356). Multiple-variable models showed statistically significant individual effects and superior diagnostic performance on ROC analysis.

CONCLUSION—TDLs can be diagnosed on preoperative MRI with a high degree of specificity; MRI features of incomplete rim enhancement, high ADC values, and a large number of lesions individually increase the probability and diagnostic confidence that a lesion is a TDL.

Address correspondence to M. C. Mabray (marc.mabray@ucsf.edu)..

Based on a presentation at the American Society of Neuroradiology 2011 annual meeting, Seattle, WA.

Keywords

apparent diffusion coefficient (ADC); diffusion; primary CNS lymphoma (PCNSL); tumefactive demyelinating lesion (TDL); tumefactive demyelination

Masslike demyelinating lesions of the brain simulating the appearance of an aggressive brain tumor, also referred to as tumefactive demyelinating lesions (TDLs), can pose a considerable diagnostic challenge [1]. On MRI, TDLs are generally larger than 2 cm and exhibit varying degrees of mass effect, contrast enhancement including irregular incomplete rim enhancement, reduced diffusion, central nonenhancement or necrosis, and surrounding edema. These conventional imaging features and clinical presentation can simulate aggressive high-grade brain tumors such as primary CNS lymphoma (PCNSL) and high-grade glioma [1–9] (Fig. 1).

The overlap in the imaging appearance of TDLs with the imaging appearances of primary brain neoplasms often leads to surgical biopsy, which may not always provide a definitive diagnosis. The lymphodepletive effect of corticosteroid therapy, which is frequently given to patients with suspected TDLs before biopsy, can obscure the histologic features of both PCNSLs and TDLs [10, 11]. Additionally, abnormal mitotic figures in reactive astrocytes within TDLs can potentially mimic high-grade gliomas on histology [12]. Corticosteroids can also further confound the diagnostic dilemma by improving the radiologic findings of both TDLs and PCNSLs [10, 11, 13].

Ideally TDLs would be diagnosed noninvasively. Advanced imaging techniques, such as perfusion MRI and MR spectroscopy, have been explored to increase the specificity of noninvasive diagnostic imaging by exploiting differences in vascularity and metabolism [14–20]. DWI has been explored in the noninvasive diagnosis of brain mass lesions and has shown particular utility in the identification of cerebral abscesses mimicking brain neoplasms [21–24]. TDLs, PCNSLs, and high-grade gliomas have been reported to show abnormalities on DWI [19, 25–30], features that we explored further in this study.

The purpose of this study was to evaluate whether apparent diffusion coefficient (ADC) values derived from routine DWI and conventional MRI features such as incomplete rim enhancement on preoperative MRI can aid in the preoperative diagnosis of TDLs and hence help avoid potential high-risk and non-diagnostic surgical tissue sampling. Our specific hypotheses were that the ADC values of TDLs differ from the ADC values of PCNSLs and high-grade gliomas and that ADC value thresholds and conventional MRI features can be used to diagnose TDLs noninvasively with a high degree of specificity.

Materials and Methods

Study Participants

Seventy-five patients (24 with TDLs, 28 with PCNSLs, 23 with high-grade gliomas) with 168 mass lesions in the brain (70 TDLs, 68 PCNSLs, and 30 high-grade gliomas) were included in this retrospective institutional review board–approved study. From 2002 to 2011, 24 patients (10 males, 14 females; mean age, 35.1 years; age range, 16–53 years) presented

with newly diagnosed TDLs at our institution; these patients constitute the TDL cohort. The TDL diagnosis was confirmed either pathologically (n = 12) or clinically (n = 12) on the basis of imaging findings, CSF analysis, and documented clinical follow-up with neurologic findings that fulfilled the revised McDonald criteria [31].

During the same time period, 28 immunocompetent patients (14 men, 14 women; mean age, 64.0 years; age range, 30–91 years) underwent preoperative MRI, and PCNSL was subsequently diagnosed at surgical biopsy (histopathologic diagnosis of diffuse B-cell PCNSL); these patients constitute the PCNSL control group.

Twenty-three consecutive patients (9 men, 14 women; mean age, 56.4 years; age range, 26–71 years) from this same time period underwent preoperative MRI and high-grade glioma was subsequently diagnosed at surgical biopsy (histopathologic diagnosis of grade IV glioblastoma); these patients were selected to constitute the high-grade glioma control group.

The exclusion criteria were a lack of preoperative MRI with DWI; an unclear or alternative diagnosis; positive HIV status; or, for the patients with PCNSL, the presence of lymphoma outside the CNS based on CT of the chest, abdomen, and pelvis.

MRI and Lesion Segmentation

A standard clinical MRI protocol was performed at 1.5 or 3 T. The protocol for the study time period was as follows: a three-plane localizer sequence, sagittal T1-weighted spin-echo sequence (TR/TE, 600/17), axial 3D T2-weighted fast spin-echo sequence (TR/TE, 3000/102), axial FLAIR sequence (TR/TE, 10,000/148; inversion time, 2200 ms), and axial DWI sequence (TR/TE, 10,000/99; section thickness, 5 mm; intersection gap, 0 mm; matrix size, 256 × 256; FOV, 24 cm; 3 orthogonal diffusion gradient directions; b values, 0 and 1000 s/mm^2) acquired in the transverse plane covering the whole brain. In addition, a contrast-enhanced 3D spoiled gradient-recalled T1-weighted imaging sequence (TR/TE, 34/8; section thickness, 1.5 mm; intersection gap, 0 mm) and axial T1-weighted contrast-enhanced spin-echo imaging sequence (TR/TE, 500/20) were performed. Slight variations in the scanning protocol were allowed as long as the patients underwent DWI performed at b values of 0 and 1000 s/mm^2 because slight changes were made in departmental protocol over time.

All image processing and analysis were performed in a blinded fashion offline from the clinical PACS workstation utilizing the FuncTool application (version 9.4.05a, GE Healthcare) of an Advantage Workstation (version 4.5, GE Health care). ADC maps were constructed from the DW images and reviewed alongside contrast-enhanced T1-weighted images, DW images, and T2-weighted FLAIR images. Each lesion was manually segmented on each slice of the ADC map by contouring the area of ADC abnormality corresponding to the entire lesion (Fig. 1). T2-weighted FLAIR images were used to exclude any adjacent edema and fluid within the ventricular system.

Minimum ADC (ADC_{min}) and average ADC (ADC_{avg}) values were calculated for each lesion volume in units of 10^{-3} mm^2/s. (All ADC values in this article are reported in units of

$\times 10^{-3}$ mm^2/s.) The number of lesions and the presence or absence of an incomplete rim pattern of contrast enhancement were recorded. To evaluate the interobserver reproducibility of these methods, a second reviewer blinded to the observations and measurements of the first reviewer rereviewed and recontoured 20 of the lesions to derive ADC_{min} and ADC_{avg} values and determine whether there was an incomplete rim pattern of contrast enhancement. All ROI measurements were performed by neuroradiology trainees and were approved by an attending neuroradiologist certified by the American Board of Radiology with a certificate of added qualification in neuroradiology.

Statistical Analyses

Statistical analyses were performed using statistics software (MedCalc for Microsoft Windows, version 14.8.1, MedCalc Software). The mean age and SD were calculated for each patient group. Mean, SD, and 95% CIs were calculated for ADC_{min} and ADC_{avg} for the TDL, PCNSL, and high-grade glioma lesion groups. To test interrater reliability over 20 lesions, we calculated Cohen's kappa for the categoric variable of the presence or absence of an incomplete rim of enhancement and calculated the concordance correlation for the continuous variables of ADC_{min} and ADC_{avg}. A one-way ANOVA was performed for both ADC_{min} and ADC_{avg} of the 168 lesions with a Tukey-Kramer pairwise comparison of each lesion type to test the hypothesis that the ADC values of TDLs differ from the ADC values of PCNSLs or high-grade gliomas.

An ROC analysis was then conducted for ADC_{min} and ADC_{avg} for the diagnosis of a TDL to test the hypothesis that ADC_{min} and ADC_{avg} thresholds could be used to diagnose a TDL. This analysis included the calculation of the AUC with testing against the null hypothesis (AUC = 0.5) and identification of the optimized threshold based on the Youden J index (i.e., the vertical distance to the null hypothesis line or sensitivity vs [1 – specificity]) and bootstrapping to generate 95% CIs. ROC analyses were also performed for the presence of an incomplete rim of contrast enhancement and for the number of lesions to predict a TDL. Multiple-variable logistic regression was then performed using the predictive variables of ADC_{min}, number of lesions, and presence of an incomplete rim pattern of contrast enhancement to diagnose a TDL. This analysis was repeated for ADC_{avg}, number of lesions, and presence of an incomplete rim pattern of contrast enhancement to diagnose a TDL and also for number of lesions and presence of an incomplete rim pattern of contrast enhancement.

Multiple-variable ROC analyses were then performed for these multiple-variable models using the same method as was used for the single-variable models. The ROC curves of the ADC_{min} and ADC_{avg} multiple-variable models were compared with the corresponding single-variable ROCs and the non-ADC multiple-variable ROCs using the ROC Compare function of MedCalc, which utilizes the DeLong method accounting for correlated variables [32]. A Hochberg posthoc correction was applied to keep an overall study alpha of 0.05. This posthoc correction indicates that all p val-ues < 0.05 in this study are statistically significant.

Results

Patient Characteristics

Seventy-five patients (24 with TDLs, 28 with PCNSLs, 23 with high-grade gliomas) with 168 mass lesions in the brain (70 TDLs, 68 PCNSLs, and 30 high-grade gliomas) were included in this study. There were 33 males and 42 females, and the mean age was 52.4 years (SD, 17.2 years; age range, 16–91 years). The TDL group included 24 patients (10 males, 14 females; age range, 16–53 years) with a mean age of 35.1 years and an SD of 9.7 years. There were 70 TDLs in the 24 patients (mean, 2.9 lesions per patient). The PCNSL group included 28 patients (14 men, 14 women; age range, 30– 91 years) with a mean age of 64.0 years and an SD of 12.4 years. There were 68 PCNSLs in the 28 patients (2.4 lesions per patient). The high-grade glioma group included 23 patients (9 men, 14 women; age range, 26–71 years) with a mean age of 56.4 years and an SD of 13.7 years. There were 30 high-grade gliomas in the 23 patients (1.3 lesions per patient).

Fifty of the 70 TDLs, 0 of the 68 PCNSLs, and 2 of the 30 high-grade gliomas showed an incomplete rim pattern of contrast enhancement. Example lesions are presented in Figure 2.

Interrater Reliability Testing

Cohen's kappa statistic was 0.894 for the presence or absence of an incomplete rim of contrast enhancement, which indicates high interrater reliability. The concordance correlation coefficient was 0.830 (Pearson correlation coefficient: $p = 0.859$) for ADC_{min} and 0.958 (Pearson correlation coefficient: $p = 0.960$) for ADC_{avg}; these results indicate high concordance.

Minimum Apparent Diffusion Coefficient by Lesion Type

The mean ADC_{min} for TDLs ($n = 70$) was 0.886 with an SD of 0.270 and a 95% CI of 0.802–0.931. The mean ADC_{min} for PCNSLs ($n = 68$) was 0.547 with an SD of 0.211 and a 95% CI of 0.496–0.598. The mean ADC_{min} for high-grade gliomas ($n = 30$) was 0.470 with an SD of 0.228 and a 95% CI of 0.385– 0.555. The ADC_{min} was statistically significantly higher for TDLs than for PCNSLs ($p < 0.01$) and high-grade gliomas ($p < 0.01$) with a one-way ANOVA (F statistic, 42.61; $p < 0.01$) using a Tukey-Kramer pairwise test. ADC_{min} was not statistically significantly different between high-grade gliomas and PCNSLs ($p > 0.05$). These results are presented as a boxplot in Figure 3.

Average Apparent Diffusion Coefficient by Lesion Type

The mean ADC_{avg} for TDLs ($n = 70$) was 1.362 with an SD of 0.395 and a 95% CI of 1.268–1.456. The mean ADC_{avg} for PCNSLs ($n = 68$) was 0.990 with an SD of 0.292 and a 95% CI of 0.919–1.061. The mean ADC_{avg} for high-grade gliomas ($n = 30$) was 1.216 with an SD of 0.380 and a 95% CI of 1.074– 1.356. ADC_{avg} was statistically significantly higher for TDLs as compared with PCNSLs ($p < 0.01$) but did not reach statistical significance when compared with high-grade gliomas ($p > 0.05$) with a one-way ANOVA (F statistic, 19.16; $p < 0.01$) using a Tukey-Kramer pairwise test. ADC_{avg} was also statistically significantly higher for high-grade gliomas as compared with PCNSLs ($p < 0.01$). These results are presented as a boxplot in Figure 4.

ROC of Minimum Apparent Diffusion Coefficient for the Diagnosis of Tumefactive Demyelinating Lesions

ROC analysis of ADC_{min} values for the diagnosis of TDLs yielded an AUC of 0.839 (95% CI, 0.774–0.891) with a $p < 0.01$. The highest Youden index J was 0.522 (95% CI, 0.385–0.614) at an ADC_{min} threshold of > 0.722 (95% CI, 0.569–0.879). This criterion (> 0.722) corresponded to a sensitivity of 0.686, a specificity of 0.837, a positive likelihood ratio of 4.20, and a negative likelihood ratio of 0.38. These results are presented in Table 1 and Figure 5.

ROC of Average Apparent Diffusion Coefficient for the Diagnosis of Tumefactive Demyelinating Lesions

ROC analysis of ADC_{avg} for the diagnosis of TDLs yielded an AUC of 0.749 (95% CI, 0.677–0.813) with a $p < 0.01$. The highest Youden index J was 0.463 (95% CI, 0.318–0.584) at an ADC_{avg} threshold of > 1.146 (95% CI, 1.129–1.403). This criterion (> 1.146) corresponded to a sensitivity of 0.729, a specificity of 0.735, a positive likelihood ratio of 2.75, and a negative likelihood ratio of 0.37. These results are presented in Table 1 and Figure 5.

Incomplete Rim Enhancement

Incomplete rim enhancement had a sensitivity of 0.714 and a specificity of 0.980 for the diagnosis of a TDL on a per-lesion basis. The positive likelihood ratio was 35.00, the negative likelihood ratio was 0.29, the Youden index J was 0.694, and the AUC was 0.854. These results are presented in Table 1 and Figure 5.

Number of Lesions

ROC analysis of the number of lesions for the diagnosis of TDLs yielded an AUC of 0.717 (95% CI, 0.643–0.784) with a $p < 0.01$. The highest Youden index J was 0.410 (95% CI, 0.266–0.531) at a diagnostic threshold of > 5 lesions (95% CI, 2–6). This criterion (> 5 lesions) corresponded to a sensitivity of 0.543, a specificity of 0.867, a positive likelihood ratio of 4.09, and a negative likelihood ratio of 0.53. These results are presented in Table 1 and Figure 5.

Multiple-Variable Logistic Regression and ROC Using Minimum Apparent Diffusion Coefficient Values

Multiple-variable logistic regression for the identification of TDLs using the predictive variables of ADC_{min}, number of leions, and the presence of an incomplete rim of contrast enhancement was statistically significant, with an overall model p value of < 0.01 (intercept = –12.74). ADC_{min} (odds ratio [OR], 36,152 [95% CI, 212.7– 6,143,451]), number of lesions (OR, 2.079 [95% CI, 1.36–3.18]), and incomplete rim enhancement (OR, 1948 [95% CI, 94.44– 40,183]) were all individually statistically significant factors.

A multiple-variable ROC analysis using this model yielded an AUC of 0.926 (95% CI, 0.875–0.961) and $p < 0.01$. The highest Youden index J was 0.794 (95% CI, 0.675– 0.869)

at a calculated probability threshold of > 0.427, which corresponded to a sensitivity of 0.814 and a specificity of 0.980. These results are presented in Table 2 and Figure 6.

Multiple-Variable Logistic Regression and ROC Using Average Apparent Diffusion Coefficient Values

Multiple-variable logistic regression for the identification of TDLs using the predictive variables of ADC_{avg}, number of lesions, and the presence of an incomplete rim of contrast enhancement was statistically significant, with an overall model p value of < 0.01 (intercept = –6.632). ADC_{avg} (OR, 9.955 [95% CI, 2.326–42.61]), number of lesions (OR, 1.740 [95% CI, 1.335–2.268]), and incomplete rim enhancement (OR, 193.3 [95% CI, 33.53–1114]) were all individually statistically significant factors.

A multiple-variable ROC analysis using this model yielded an AUC of 0.954 (95% CI, 0.957–0.988) and $p < 0.01$. The highest Youden index J was 0.855 (95% CI, 0.742– 0.910) at a calculated probability threshold of > 0.362, which corresponded to a sensitivity of 0.886 and a specificity of 0.969. These results are presented in Table 2 and Figure 6.

Multiple-Variable Logistic Regression and ROC Using Incomplete Rim Enhancement and Number of Lesions

Multiple-variable logistic regression for the identification of TDLs using the predictive variables of the presence of an incomplete rim of contrast enhancement and number of lesions was statistically significant, with an overall model p value of < 0.01 (intercept = –3.716). Incomplete rim enhancement (OR, 207.8 [95% CI, 39.09–1104]) and number of lesions (OR, 1.631 [95% CI, 1.30– 2.04]) were both individually statistically significant factors.

A multiple-variable ROC analysis using this model yielded an AUC of 0.986 (95% CI, 0.954–0.998) and $p < 0.01$. The highest Youden index J was 0.863 (95% CI, 0.765– 0.900) at a calculated probability threshold of > 0.501, which corresponded to a sensitivity of 0.914 and a specificity of 0.949. These results are presented in Table 2 and Figure 6.

ROC Comparisons

The multiple-variable model ROC using ADC_{min} (AUC = 0.986) was statistically significantly superior to the ROC using incomplete rim enhancement (AUC = 0.854, $p < 0.01$), the ROC using number of lesions (AUC = 0.717, $p < 0.01$), the ROC using ADC_{min} (AUC = 0.839, $p < 0.01$), and the ROC using incomplete rim enhancement and number of lesions (AUC = 0.926, $p < 0.01$).

The multiple-variable model ROC using ADC_{avg} (AUC = 0.954) was statistically significantly superior to the ROC using incomplete rim enhancement (AUC = 0.854, $p < 0.01$), the ROC using number of lesions (AUC = 0.717, $p < 0.01$), the ROC using ADC_{avg} (AUC = 0.749, $p < 0.01$), and the ROC using incomplete rim enhancement and number of lesions (AUC = 0.926, $p = 0.025$). These results are presented in Table 3.

Discussion

The results of our study show that ADC values and conventional MRI features can be used to help differentiate TDLs from brain neoplasms with a high degree of specificity. Although TDLs, PCNSLs, and high-grade gliomas can all have areas of reduced diffusion, our study shows that the ADC values of TDLs differ from those of PCNSLs and high-grade gliomas. Specifically, ADC_{min} values were higher in TDLs than in PCNSLs or high-grade gliomas and ADC_{avg} values were higher in TDLs than in PCNSLs but not in high-grade gliomas. Both ADC_{min} and ADC_{avg} performed well in their stand alone ability to diagnose TDLs in this study as did the number of lesions and incomplete rim enhancement; incomplete rim enhancement notably had the highest specificity of the tested single variables (98.0%). Diagnostic performance was statistically significantly augmented when these variables were considered in multiple-variable models with statistically significant individual effects for all tested variables. Our study shows that TDLs can be diagnosed with a high degree of specificity on preoperative MRI and that incomplete rim enhancement, a large number of lesions, and high ADC values should all individually increase diagnostic confidence that a lesion is a TDL.

There are well-established imaging and clinical features that suggest a brain mass is more likely to be a TDL: relatively little mass effect and edema compared with lesion size, rim or incomplete rim enhancement, dilated veins within the lesion, and responsiveness to corticosteroid therapy [1, 13, 14, 33–35]. Nevertheless, many patients undergo surgical biopsy because these features are neither completely sensitive nor specific [10, 11, 36– 38]. Even on histopathology, TDLs can be confused for aggressive tumors such as high-grade gliomas because of atypical reactive astrocytes with mitotic figures [12]. Biopsy specimens of PCNSLs may also be nondiag-nostic, and imaging findings of PCNSLs may also respond to corticosteroids because of the lymphodepletive effect of corticosteroid therapy, potentially further confounding the clinical situation [10, 11]. Performing preoperative imaging for diagnosis is preferable to surgical biopsy if possible.

In the past decade, advanced imaging techniques have been explored to improve the noninvasive diagnostic accuracy of these techniques for TDLs; most of these imaging techniques focus on differentiation of TDLs from high-grade gliomas. Specifically, perfusion MRI and MR spectroscopy are helpful to discriminate lesions on the basis of lesion vascularity and metabolism, respectively [13–19]. Using dynamic susceptibility contrast-enhanced MRI, Cha et al. [14] showed significant differences in cerebral blood volume (CBV) values between TDLs and intracranial neoplasms, with greatest CBV values for high-grade glial tumors that show profound angiogenesis. Although the difference in CBV values was still statistically significant, the difference was less pronounced for the four patients with PCNSLs included in that study [14].

Reduced ADC values in PCNSLs and high-grade gliomas are related to tumor cellularity [39, 40]. The basis of reduced ADC values in TDLs is likely infiltration of inflammatory cells within the lesion; however, TDLs are generally hypocellular lesions, and overall the lesions show heterogeneity of ADC values [19, 25–27]. The lower ADC values and more homogeneous reduced ADCs in the PCNSLs as opposed to the TDLs on imaging correspond

to our understanding of the pathology: Compared with TDLs, PCNSLs are more cellular lesions and TDLs are more heterogeneous lesions that are characterized by an area of disruption of the blood-brain barrier, inflammatory cell infiltration, myelin damage, and a large component of adjacent edema. This heterogeneous “leading edge” pathologic finding is likely the basis for the peripheral rim pattern of reduced ADCs that was seen in some of the TDL cases in our study; this feature has been described previously and is similar to the previously described incomplete rim pattern of enhancement, the so-called “open ring,” that was frequently encountered in the TDL cases in our study [19, 22, 23]. The high-grade gliomas in our study showed low ADC values, particularly ADC_{min} values, which is likely related to the high cellularity of these lesions. However, the ADC_{avg} values in high-grade gliomas were elevated and were similar to the values seen in TDLs; this similarity was likely the result of including cystic and necrotic areas of the high-grade gliomas and reflects the heterogeneous nature of these tumors.

The diagnostic performance as evaluated by ROC analysis was reasonably good (AUC = 0.717–0.854) for all of the four single variables tested but was excellent (AUC = 0.954–0.986) and was statistically significantly superior for the multiple-variable models incorporating ADC values. The results of our multiple-variable logistic regression models showed statistically significant individual effects for all of the individual variables in the models. These results show that each variable had a statistically significant impact on the probability of a lesion being a TDL after the other variables had been accounted for and provides a statistical basis for factoring all of these variables into the diagnostic confidence that a lesion is a TDL. Incomplete rim enhancement was highly specific for the diagnosis of TDLs in our study (98.0% specificity); however, the results of multiple-variable analyses do show an overall statistically significant added benefit by considering the other variables as well. We also evaluated a multiple-variable model without ADC, incorporating the number of lesions and incomplete rim enhancement which was also excellent in the prediction of TDLs (AUC = 0.926); however, adding ADC into the analysis led to statistically significantly better diagnostic performance. Overall the results of our analysis should be considered to show that it is possible to diagnose TDLs on preoperative MRI with a high degree of specificity and that incomplete rim enhancement, high ADC values, and a large number of lesions should all individually increase diagnostic confidence that a lesion is a TDL.

The limitations of our study include the relatively modest sample size and the retrospective nature of the study. We used a retrospective case-control design for our study because TDLs are relatively rare compared with brain tumors such as high-grade gliomas. Although this study provides insights into differences in ADC characteristics of these lesions that could be used clinically, the clinical feasibility of replicating our study with measurements of ADC would present a challenge to clinical workflow; however, we routinely use a similar processing method in daily practice for the perfusion analysis.

Possible future directions of research to make the quantitative technique more easily clinically applicable could include testing the performance of clinical workstation–derived relative ADC values on preprocessed ADC maps with a single ROI. Prior research has suggested that it may be possible to derive accurate ADC values on a standard clinical

workstation in liver lesions [41]. This strategy could potentially be evaluated in the context of TDLs; however, this strategy would be unlikely to perform as well as the carefully manually defined ROIs used in our study, particularly because the workstation would derive only a single-slice ADC_{avg} value. The reproducibility of our ADC analysis based on manually drawn ROIs may also be a potential limitation, although interrater testing suggested an acceptable concordance. Future studies could evaluate the use of automatically segmented lesions and potential applications to computer-aided diagnosis using ADC values and the additional variables that we included in our model. With regard to our multiple-variable analyses, these models are limited by the choice of variables, which were limited for the sake of simplicity.

MR spectroscopy and perfusion MRI data were not included in our analysis because these techniques were not routinely performed. Subjectively dilated venous structures were also not evaluated because these findings were not frequently encountered. Age was identified as a statistically significant factor, with the TDL patients being younger than the non-TDL patients; however, this variable was excluded from multiple-variable analysis to focus solely on variables derived from the preoperative MRI examinations.

In conclusion, the results of our study show that preoperative MRI can be used to diagnose TDLs with a high degree of specificity. We have reported that TDLs show statistically significantly higher ADC_{min} and ADC_{avg} values than PCNSLs ($p < 0.01$) and higher ADC_{min} values than high-grade gliomas ($p < 0.01$) in our study of 168 brain mass lesions. ADC_{min} (AUC = 0.839) and ADC_{avg} (AUC = 0.749) values had acceptable performance in ROC analysis for the identification of TDLs, as did the number of lesions (AUC = 0.717) and incomplete rim enhancement (AUC = 0.854). Incomplete rim enhancement notably had a very high degree of specificity (98.0%) for the diagnosis of TDLs. Multiple-variable analyses including ADC values showed statistically significant individual effects for ADC (as ADC_{min} or ADC_{avg}), number of lesions, and incomplete rim enhancement and statistically significantly superior diagnostic performance on ROC analysis (AUC = 0.954–0.986) as compared with single-variable models and non-ADC models. These results suggest that it is possible to diagnose TDLs on preoperative MRI with a high degree of specificity and that incomplete rim enhancement, high ADC values, and a large number of lesions should all individually increase diagnostic confidence that a lesion is a TDL. These results may potentially be used in the future to avoid surgical tissue sampling.

Acknowledgments

M. C. Mabray was supported by a National Institutes of Health training grant (5T32EB001631-10).

References

1. Dagher AP, Smirniotopoulos J. Tumefactive demyelinating lesions. Neuroradiology. 1996; 38:560–565. [PubMed: 8880719]
2. van der Velden M, Bots GT, Endtz LJ. Cranial CT in multiple sclerosis showing a mass effect. Surg Neurol. 1979; 12:307–310. [PubMed: 524246]
3. Rieth KG, Di Chiro G, Cromwell LD, et al. Primary demyelinating disease simulating glioma of the corpus callosum: report of three cases. J Neurosurg. 1981; 55:620–624. [PubMed: 7277009]

4. Sagar HJ, Warlow CP, Sheldon PW, Esiri MM. Multiple sclerosis with clinical and radiological features of cerebral tumour. J Neurol Neurosurg Psychiatry. 1982; 45:802–808. [PubMed: 7131013]
5. Wang AM, Morris JH, Hickey WF, Hammerschlag SB, O'Reilly GV, Rumbaugh CL. Unusual CT patterns of multiple sclerosis. AJNR. 1983; 4:47–50. [PubMed: 6402902]
6. Kalyan-Raman UP, Garwacki DJ, Elwood PW. Demyelinating disease of corpus callosum presenting as glioma on magnetic resonance scan: a case documented with pathological findings. Neurosurgery. 1987; 21:247–250. [PubMed: 3658137]
7. Hunter SB, Ballinger WE Jr, Rubin JJ. Multiple sclerosis mimicking primary brain tumor. Arch Pathol Lab Med. 1987; 111:464–468. [PubMed: 3566474]
8. Youl BD, Kermode AG, Thompson AJ, et al. Destructive lesions in demyelinating disease. J Neurol Neurosurg Psychiatry. 1991; 54:288–292. [PubMed: 2056314]
9. Giang DW, Poduri KR, Eskin TA, et al. Multiple sclerosis masquerading as a mass lesion. Neuroradiology. 1992; 34:150–154. [PubMed: 1603315]
10. Geppert M, Ostertag CB, Seitz G, Kiessling M. Glucocorticoid therapy obscures the diagnosis of cerebral lymphoma. Acta Neuropathol. 1990; 80:629–634. [PubMed: 2275339]
11. Weller M. Glucocorticoid treatment of primary CNS lymphoma. J Neurooncol. 1999; 43:237–239. [PubMed: 10563429]
12. Zagzag D, Miller DC, Kleinman GM, Abati A, Donnenfeld H, Budzilovich GN. Demyelinating disease versus tumor in surgical neuropathology: clues to a correct pathological diagnosis. Am J Surg Pathol. 1993; 17:537–545. [PubMed: 8333553]
13. Kepes JJ. Large focal tumor-like demyelinating lesions of the brain: intermediate entity between multiple sclerosis and acute disseminated encephalomyelitis? A study of 31 patients. Ann Neurol. 1993; 33:18–27. [PubMed: 8494332]
14. Cha S, Pierce S, Knopp EA, et al. Dynamic contrast-enhanced T2*-weighted MR imaging of tumefactive demyelinating lesions. AJNR. 2001; 22:1109–1116. [PubMed: 11415906]
15. Saindane AM, Cha S, Law M, Xue X, Knopp EA, Zagzag D. Proton MR spectroscopy of tumefactive demyelinating lesions. AJNR. 2002; 23:1378–1386. [PubMed: 12223381]
16. Law M, Meltzer DE, Cha S. Spectroscopic magnetic resonance imaging of a tumefactive demyelinating lesion. Neuroradiology. 2002; 44:986–989. [PubMed: 12483443]
17. Enzinger C, Strasser-Fuchs S, Ropele S, Kapeller P, Kleinert R, Fazekas F. Tumefactive demyelinating lesions: conventional and advanced magnetic resonance imaging. Mult Scler. 2005; 11:135–139. [PubMed: 15794384]
18. Cianfoni A, Niku S, Imbesi SG. Metabolite findings in tumefactive demyelinating lesions utilizing short echo time proton magnetic resonance spectroscopy. AJNR. 2007; 28:272–277. [PubMed: 17296993]
19. Malhotra HS, Jain KK, Agarwal A, et al. Characterization of tumefactive demyelinating lesions using MR imaging and in-vivo proton MR spectroscopy. Mult Scler. 2009; 15:193–203. [PubMed: 19181773]
20. Blasel S, Pfeilschifter W, Jansen V, Mueller K, Zanella F, Hattingen E. Metabolism and regional cerebral blood volume in autoimmune inflammatory demyelinating lesions mimicking malignant gliomas. J Neurol. 2011; 258:113–122. [PubMed: 20803026]
21. Tung GA, Evangelista P, Rogg JM, Duncan JA 3rd. Diffusion-weighted MR imaging of rim-enhancing brain masses: is markedly decreased water diffusion specific for brain abscess? AJR. 2001; 177:709–712. [PubMed: 11517080]
22. Desprechins B, Stadnik T, Koerts G, Shabana W, Breucq C, Osteaux M. Use of diffusion-weighted MR imaging in differential diagnosis between intracerebral necrotic tumors and cerebral abscesses. AJNR. 1999; 20:1252–1257. [PubMed: 10472982]
23. Stadnik TW, Chaskis C, Michotte A, et al. Diffusion-weighted MR imaging of intracerebral masses: comparison with conventional MR imaging and histologic findings. AJNR. 2001; 22:969–976. [PubMed: 11337344]
24. Ebisu T, Tanaka C, Umeda M, et al. Discrimination of brain abscess from necrotic or cystic tumors by diffusion-weighted echo planar imaging. Magn Reson Imaging. 1996; 14:1113–1116. [PubMed: 9071004]

25. Bernarding J, Braun J, Koennecke HC. Diffusion- and perfusion-weighted MR imaging in a patient with acute demyelinating encephalomyelitis (ADEM). J Magn Reson Imaging. 2002; 15:96–100. [PubMed: 11793463]
26. Ernst T, Chang L, Walot I, Huff K. Physiologic MRI of a tumefactive multiple sclerosis lesion. Neurology. 1998; 51:1486–1488. [PubMed: 9818892]
27. Rovaris M, Gass A, Bammer R, et al. Diffusion MRI in multiple sclerosis. Neurology. 2005; 65:1526–1532. [PubMed: 16301477]
28. Horger M, Fenchel M, Nagele T, et al. Water diffusivity: comparison of primary CNS lymphoma and astrocytic tumor infiltrating the corpus callosum. AJR. 2009; 193:1384–1387. [PubMed: 19843757]
29. Zacharia TT, Law M, Naidich TP, Leeds NE. Central nervous system lymphoma characterization by diffusion-weighted imaging and MR spectroscopy. J Neuroimaging. 2008; 18:411–417. [PubMed: 18494774]
30. Toh CH, Castillo M, Wong AM, et al. Primary cerebral lymphoma and glioblastoma multiforme: differences in diffusion characteristics evaluated with diffusion tensor imaging. AJNR. 2008; 29:471–475. [PubMed: 18065516]
31. Polman CH, Reingold SC, Banwell B, et al. Diagnostic criteria for multiple sclerosis: 2010 revisions to the McDonald criteria. Ann Neurol. 2011; 69:292–302. [PubMed: 21387374]
32. DeLong ER, DeLong DM, Clarke-Pearson DL. Comparing the areas under two or more correlated receiver operating characteristic curves: a nonparametric approach. Biometrics. 1988; 44:837–845. [PubMed: 3203132]
33. Given CA 2nd, Stevens BS, Lee C. The MRI appearance of tumefactive demyelinating lesions. AJR. 2004; 182:195–199. [PubMed: 14684539]
34. Masdeu JC, Moreira J, Trasi S, Visintainer P, Cavaliere R, Grundman M. The open ring: a new imaging sign in demyelinating disease. J Neuroimaging. 1996; 6:104–107. [PubMed: 8634482]
35. Masdeu JC, Quinto C, Olivera C, Tenner M, Leslie D, Visintainer P. Open-ring imaging sign: highly specific for atypical brain demyelination. Neurology. 2000; 54:1427–1433. [PubMed: 10751251]
36. Johnson BA, Fram EK, Johnson PC, Jacobowitz R. The variable MR appearance of primary lymphoma of the central nervous system: comparison with histopathologic features. AJNR. 1997; 18:563–572. [PubMed: 9090424]
37. Zhang D, Hu LB, Henning TD, et al. MRI findings of primary CNS lymphoma in 26 immunocompetent patients. Korean J Radiol. 2010; 11:269–277. [PubMed: 20461180]
38. Smirniotopoulos JG, Murphy FM, Rushing EJ, Rees JH, Schroeder JW. Patterns of contrast enhancement in the brain and meninges. RadioGraphics. 2007; 27:525–551. [PubMed: 17374867]
39. Barajas RF Jr, Rubenstein JL, Chang JS, Hwang J, Cha S. Diffusion-weighted MR imaging derived apparent diffusion coefficient is predictive of clinical outcome in primary central nervous system lymphoma. AJNR. 2010; 31:60–66. [PubMed: 19729544]
40. Guo AC, Cummings TJ, Dash RC, Provenzale JM. Lymphomas and high-grade astrocytomas: comparison of water diffusibility and histologic characteristics. Radiology. 2002; 224:177–183. [PubMed: 12091680]
41. El Kady RM, Choudhary AK, Tappouni R. Accuracy of apparent diffusion coefficient value measurement on PACS workstation: a comparative analysis. AJR. 2011; 196:W280–W284. [web]. [PubMed: 21343475]

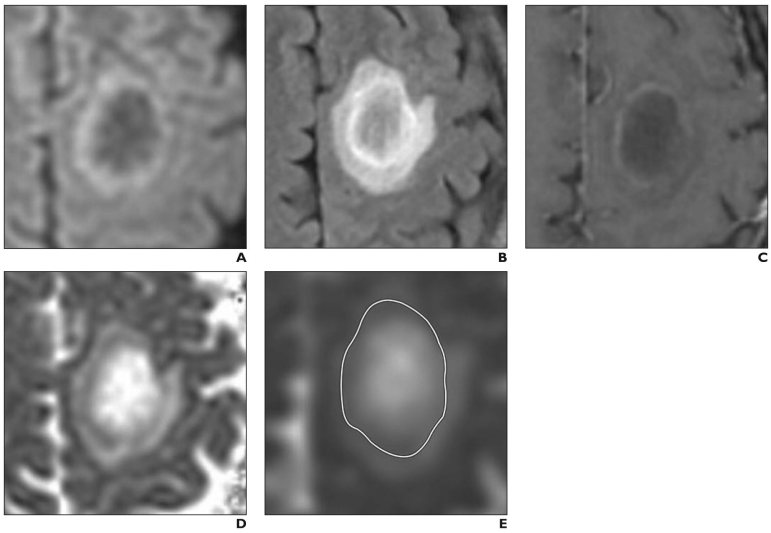

Fig. 1.

MRI of 36-year-old man with tumefactive demyelinating lesion (TDL). **A–E,** Axial DW image (**A**), axial T2-weighted FLAIR image (**B**), axial gadolinium-enhanced T1-weighted image (**C**), axial apparent diffusion coefficient (ADC) map (**D**), and axial ADC map (**E**) with ROI (*outline*, **E**) drawn on it after review of all images. ROI was drawn to include whole lesion and includes rim of reduced diffusion seen on DW image (**A**) and ADC maps (**D** and **E**) and corresponding to incomplete rim of contrast enhancement seen on gadolinium enhanced T1-weighted image (**C**). Minimum ADC (ADC_{min}) measured 0.764, and average ADC (ADC_{avg}) measured 1.620. Relatively younger age of patient and high ADC_{min}, high ADC_{avg}, and incomplete rim of contrast enhancement all suggest TDL. Diagnosis of TDL was proven at biopsy.

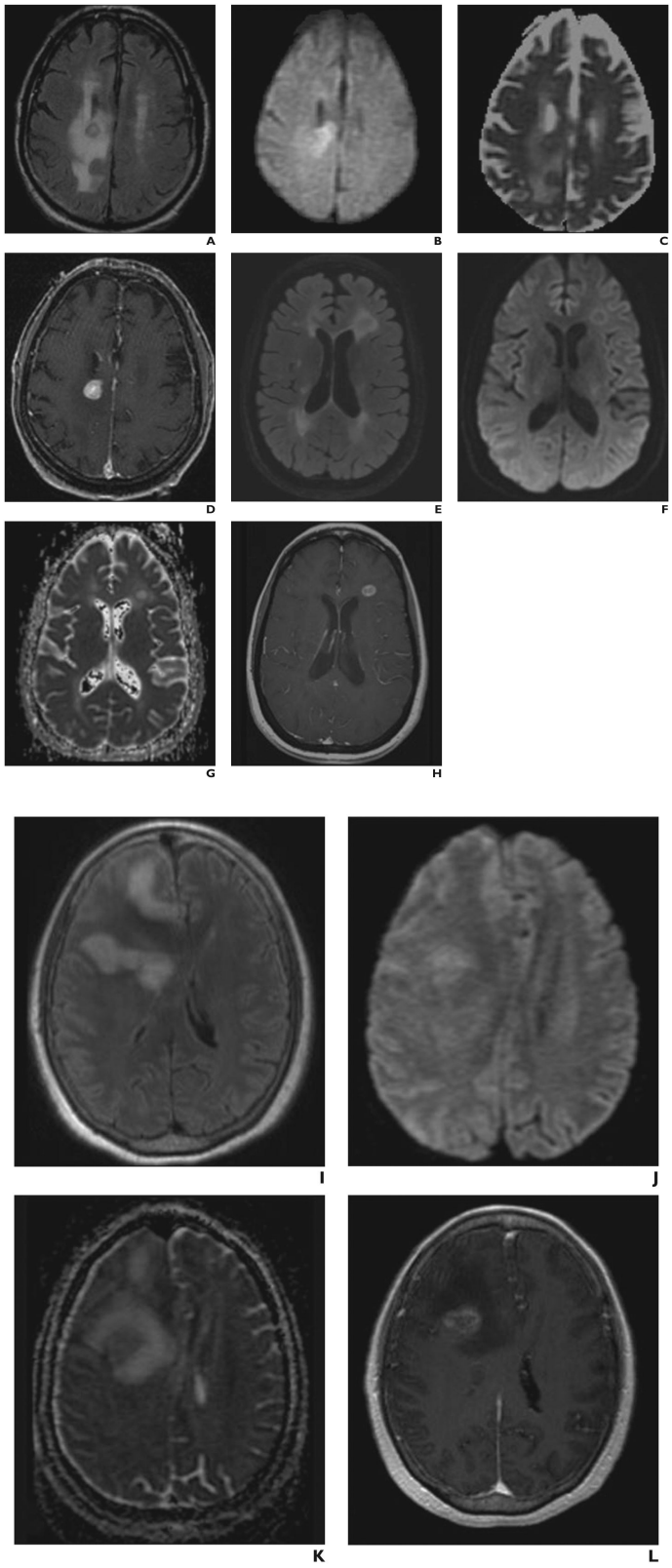

Fig. 2.

MRI of tumefactive demyelinating lesions (TDLs) and brain neoplasms. Axial T2 FLAIR (**A**), axial DWI (**B**), axial ADC map (**C**), and axial post-gadolinium T1 (**D**) MR images from an 88 year old female patient with biopsy proven primary central nervous system lymphoma. Note the corresponding relatively low ADC values visible on the ADC map (**C**). ADC_{min} measured 0.580 and ADC_{avg} measured 1.067, supporting the diagnosis. Axial T2 FLAIR (**E**), axial DWI (**F**), axial ADC map (**G**), and axial post-gadolinium T1 (**H**) MR images from a 45 year old female patient with a tumefactive demyelinating lesion. Note the corresponding relatively high ADC values visible on the ADC map (**G**). ADC_{min} measured 1.150 and ADC_{avg} measured 1.460, supporting the diagnosis. Axial T2 FLAIR (**I**), axial DWI (**J**), axial ADC map (**K**), and axial post-gadolinium T1 (**L**) MR images from a 71 year old female patient with biopsy proven glioblastoma. Note the corresponding relatively low ADC values visible on the ADC map. ADC_{min} measured 0.431 and ADC_{avg} measured 1.399 consistent with the results of our study.

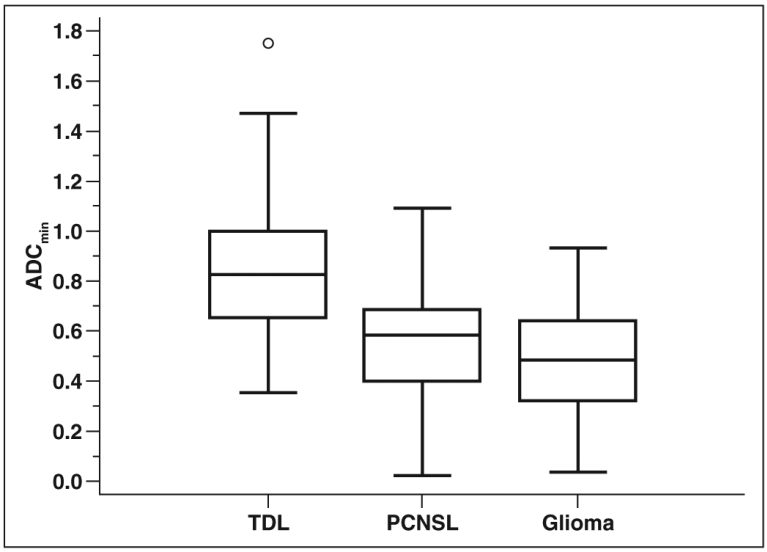

Fig. 3.

Boxplot of minimum apparent diffusion coefficient (ADC_{min}) values for each lesion group. ADC_{min} values are statistically significantly higher for tumefactive demyelinating lesions (TDLs) than for primary CNS lymphomas (PCNSLs) ($p < 0.01$) and high-grade gliomas ($p < 0.01$) with one-way ANOVA using Tukey-Kramer pairwise test. Box centered at mean ADC_{min}; middle line in boxes = median ADC_{min}; upper and lower lines of boxes = upper and lower quartiles, respectively; whiskers = highest value to lowest value excluding any statistical outliers; circle = outside value, greater than upper quartile plus 1.5 times interquartile range.

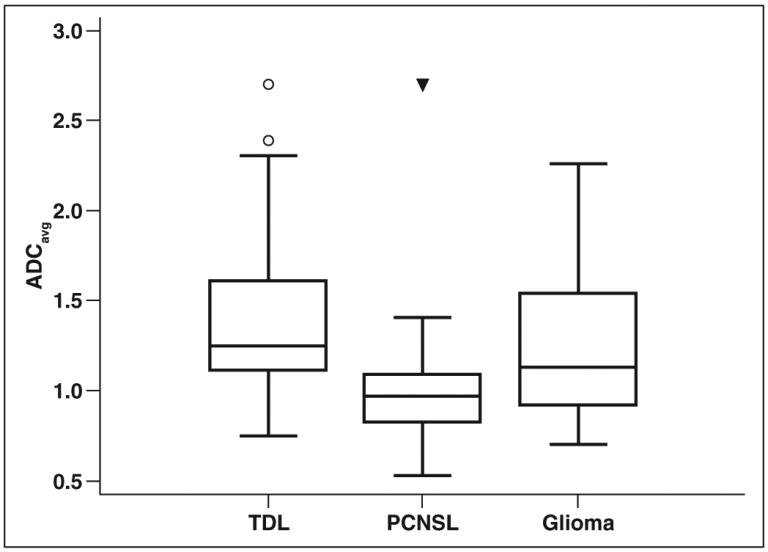

Fig. 4.

Boxplot of average apparent diffusion coefficient (ADC_{avg}) values for each lesion group. ADC_{avg} values are statistically significantly higher for tumefactive demyelinating lesions (TDLs) than for primary CNS lymphomas (PCNSLs) ($p < 0.01$) but not for high-grade gliomas ($p > 0.05$) with one-way ANOVA using Tukey-Kramer pairwise test. Box centered at mean ADC_{avg}; middle line in boxes = median ADC_{avg}; upper and lower lines of boxes = upper and lower quartiles, respectively; whiskers = highest value to lowest value excluding any statistical outliers; circle = outside value, greater than upper quartile plus 1.5 times interquartile range; triangle = far out value, greater than upper quartile plus 3 times interquartile range.

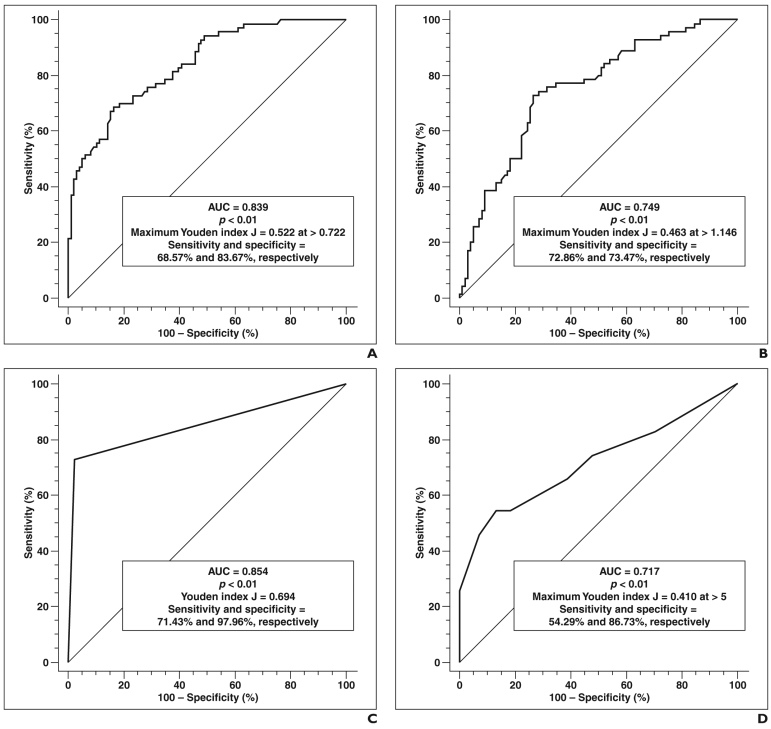

Fig. 5.

Performance of single-variable models for diagnosis of tumefactive demyelinating lesions (TDLs). Youden index J is defined as sensitivity − (1 −specificity) and is highest vertical distance from line where AUC > 0.5 (diagonal line). A, Graph shows results of ROC analysis using minimum apparent diffusion coefficient (ADC_{min}) to diagnose TDLs. B, Graph shows results of ROC analysis using average ADC (ADC_{avg}) to diagnose TDLs. C, Graph shows results of ROC analysis using incomplete rim enhancement to diagnose TDLs. D, Graph shows results of ROC analysis using number of lesions to diagnose TDLs.

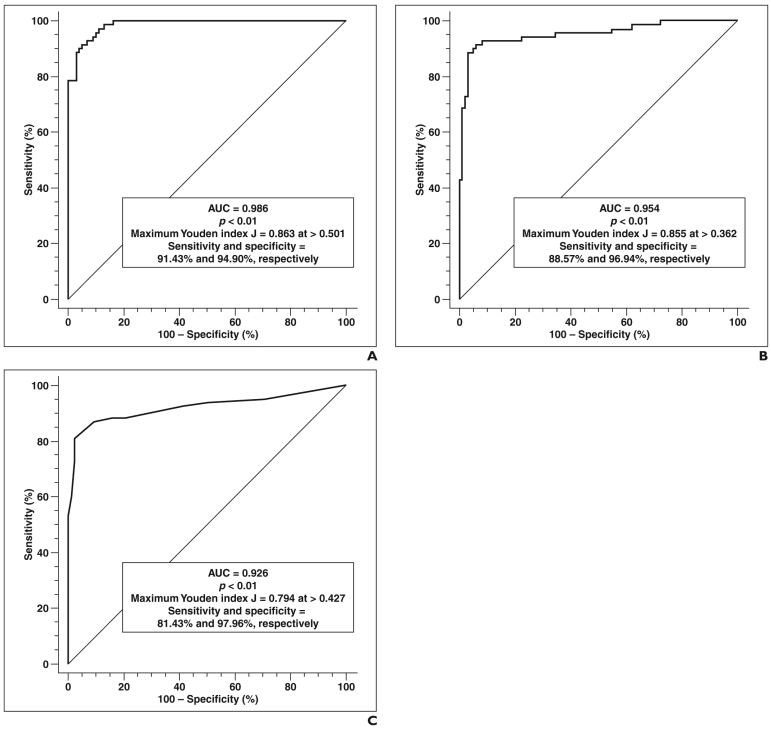

Fig. 6.

Performance of multiple-variable models for diagnosis of tumefactive demyelinating lesions (TDLs). Youden index J is defined as sensitivity −(1 − specificity) and is highest vertical distance from line where AUC > 0.5 (diagonal line). Thresholds refer to calculated probabilities from logistic regression equations. **A**, Graph shows results of ROC analysis using minimum apparent diffusion coefficient (ADC_{min}), incomplete rim enhancement, and number of lesions to diagnose TDLs. **B**, Graph shows results of ROC analysis using average ADC (ADC_{avg}), incomplete rim enhancement, and number of lesions to diagnose TDLs. **C**, Graph shows results of ROC analysis using incomplete rim enhancement and number of lesions to diagnose TDLs.

TABLE 1

Results of ROC Analyses Using Minimum Apparent Diffusion Coefficient (ADC_{min}), Average ADC (ADC_{avg}), Number of Lesions, or Incomplete Rim Enhancement for the Diagnosis of Tumefactive Demyelinating Lesions

Variable Used for ROC Analysis	AUC (95% CI)	*p*	Threshold Derivation[a] (Highest Youden Index)	Optimized Threshold	Values at Threshold (95% CI)			
					Sensitivity	Specificity	Positive Likelihood Ratio	Negative Likelihood Ratio
ADC_{min}	0.839 (0.774–0.891)	< 0.01	0.522[a]	ADC_{min} > 0.722	0.686 (0.549–0.779)	0.837 (0.748–0.904)	4.20 (2.6–6.8)	0.38 (0.3–0.5)
ADC_{avg}	0.749 (0.677–0.813)	< 0.01	0.463[a]	ADC_{avg} > 1.146	0.729 (0.609–0.828)	0.735 (0.636–0.819)	2.75 (1.9–3.9)	0.37 (0.2–0.6)
No. of lesions	0.717 (0.643–0.784)	< 0.01	0.410[a]	> 5 Lesions	0.543 (0.419–0.663)	0.867 (0.784–0.927)	4.09 (2.4–7.1)	0.53 (0.4–0.7)
Incomplete rim enhancement	0.854 (0.791–0.904)	< 0.01	0.694[b]	Present	0.714 (0.594–0.816)	0.980 (0.928–0.998)	35.00 (8.8–139)	0.29 (0.2–0.5)

[a] Highest Youden index J.

[b] Youden index J.

TABLE 2

Results of Multiple-Variable Logistic Regression Using Incomplete Rim Enhancement and Number of Lesions Alone or in Combination With Minimum Apparent Diffusion Coefficient (ADC_{min}) or Average ADC (ADC_{avg}) for the Diagnosis of Tumefactive Demyelinating Lesions (TDLs)

Factor	Effect	*p*	Odds Ratio
Multiple-variable logistic regression with ADC_{min} for identification of a TDL[a]			
ADC_{min}	10.50	< 0.01	36,152
No. of lesions	0.731	< 0.01	2.079
Incomplete rim enhancement	7.57	< 0.01	1948
Multiple-variable logistic regression with ADC_{avg} for identification of a TDL[b]			
ADC_{avg}	2.30	< 0.01	9.955
No. of lesions	0.554	< 0.01	1.740
Incomplete rim enhancement	5.26	< 0.01	193.3
Multiple-variable logistic regression with incomplete rim enhancement and no. of lesions (no ADC) for identification of a TDL[c]			
No. of lesions	0.489	< 0.01	1.631
Incomplete rim enhancement	5.34	< 0.01	207.8

Note—All variables have statistically significant effects in the models, which indicates that they are statistically significant factors for identifying TDLs and that all should be factored into diagnostic confidence.

[a] Overall model: $p < 0.01$, intercept = −12.74, AUC = 0.986.

[b] Overall model: $p < 0.01$, intercept = –6.63, AUC = 0.954.

[c] Overall model: $p < 0.01$, intercept = –3.72, AUC = 0.926.

TABLE 3

Comparisons of the Multiple-Variable Apparent Diffusion Coefficient (ADC) ROCs With the Single-Variable ROCs and the Multiple-Variable Non-ADC ROCs

Model (AUC)	*p* (AUC)			
	Corresponding ADC	No. of Lesions (0.717)	Incomplete Rim Enhancement (0.854)	No. of Lesions and Incomplete Rim Enhancement (0.926)
ADC_{min}, no. of lesions, incomplete rim enhancement (0.986)	ADC_{min}: < 0.01 (0.839)	< 0.01	< 0.01	< 0.01
ADC_{avg}, no. of lesions, incomplete rim enhancement (0.954)	ADC_{avg}: < 0.01 (0.749)	< 0.01	< 0.01	0.025

Note—The multiple-variable ADC ROCs showed statistically significantly larger AUCs, which indicate statistically significantly superior diagnostic performance.